

Cite this: *Chem. Sci.*, 2020, 11, 3829

All publication charges for this article have been paid for by the Royal Society of Chemistry

# Interfering in apoptosis and DNA repair of cancer cells to conquer cisplatin resistance by platinum(IV) prodrugs†

Shuren Zhang,<sup>a</sup> Xuanmeng Zhong,<sup>a</sup> Hao Yuan,<sup>a</sup> Yan Guo,<sup>a</sup> Dongfan Song,<sup>a</sup> Fen Qi,<sup>a</sup> Zhenzhu Zhu,<sup>c</sup> Xiaoyong Wang<sup>ib</sup>\*<sup>b</sup> and Zijian Guo<sup>ib</sup>\*<sup>a</sup>

The dysregulation of apoptosis and DNA damage repair are two leading mechanisms of cisplatin resistance. Two anticancer Pt<sup>IV</sup> prodrugs with the formulas [Pt(NH<sub>3</sub>)<sub>2</sub>Cl<sub>2</sub>(L<sub>1</sub>)<sub>2</sub>] (**1**, L<sub>1</sub> = 3-chloro-benzo[*b*]thiophene-2-carboxylic acid) and [Pt(NH<sub>3</sub>)<sub>2</sub>Cl<sub>2</sub>(L<sub>2</sub>)<sub>2</sub>] (**2**, L<sub>2</sub> = 3-chloro-6-methylbenzo[*b*]thiophene-2-carboxylic acid) were designed to target myeloid cell leukemia-1 (Mcl-1), a protein responsible for inhibiting apoptosis and promoting DNA damage repair. Complexes **1** and **2** exhibited high cytotoxicity against various cancer cell lines, especially cisplatin-resistant non-small-cell lung and ovarian cancer cells. The resistance factors of both complexes for cisplatin-resistant cancer cells also decreased markedly as compared with that of cisplatin. Both **1** and **2** could enter cancer cells effectively and cause DNA damage while simultaneously downregulating Mcl-1 to prompt a conspicuous apoptotic response. Complex **2** also downregulated the DNA damage repair proteins RAD51 and BRCA2 as well as inhibited the formation of RAD51 foci, which is regarded as a critical step and functional biomarker in homologous recombination. The acute toxicity of **1** and **2** to mice is lower than that of cisplatin, and more importantly, they show much stronger inhibition towards the growth of non-small-cell lung cancer in nude mice than cisplatin. Complexes **1** and **2** are the first Mcl-1-targeted Pt<sup>IV</sup> prodrugs, and the latter could synchronously inhibit apoptosis and DNA repair related proteins in cisplatin-resistant cancer cells. The strategy of tuning both apoptosis and DNA repair pathways opens a promising window to overcoming resistance to cisplatin in anticancer chemotherapy, and is also a breakthrough in the design of multitargeted platinum-based anticancer drugs.

Received 13th January 2020  
Accepted 20th February 2020

DOI: 10.1039/d0sc00197j

rsc.li/chemical-science

## Introduction

Cisplatin (CDDP) is one of the most effective anticancer drugs for treating various malignancies.<sup>1,2</sup> It kills cancer cells primarily through damaging nuclear DNA to trigger apoptosis,<sup>3</sup> unfortunately, its therapeutic efficacy is severely hindered by inherent and acquired drug resistance.<sup>4,5</sup> In general, CDDP resistance is multifactorial, that is, it relies on the activation of multiple molecular or cellular responses.<sup>6,7</sup> In these events, impeded apoptosis and enhanced DNA damage repair are two

vital factors because some important proteins are dysregulated in CDDP-resistant tumors.<sup>6–9</sup> For example, myeloid cell leukemia-1 (Mcl-1) is an antiapoptotic protein in the Bcl-2 family, which inhibits the progression of apoptosis *via* sequestering the proapoptotic proteins.<sup>10</sup> Overexpression of Mcl-1 is the hallmark of several cancers and is associated with drug resistance and tumor relapse.<sup>11,12</sup> Cancer cells can avoid apoptosis elicited by CDDP-mediated DNA damage through upregulating Mcl-1, leading to drug resistance;<sup>13,14</sup> whereas the depletion of Mcl-1 can impair homologous recombination (HR),<sup>15</sup> which is a major way to repair the DNA double-strand breaks (DSBs) triggered by CDDP.<sup>16,17</sup> Therefore, impaired HR can block the repair of DNA DSBs and increase the curative effect of CDDP. We suppose that targeting Mcl-1 may not only promote apoptosis *via* mediating apoptosis-related pathways, but also interfere with DNA damage repair and ultimately potentiate CDDP towards CDDP-resistant tumors.

Octahedral Pt<sup>IV</sup> prodrugs are kinetically inert in blood plasma and can be activated by biological reductants in tumor cells, such as ascorbic acid (AsA) and glutathione (GSH), producing Pt<sup>II</sup> species to damage DNA and kill cancer cells.<sup>18,19</sup> In addition to avoiding side reactions with biomolecules prior

<sup>a</sup>State Key Laboratory of Coordination Chemistry, School of Chemistry and Chemical Engineering, Chemistry and Biomedicine Innovation Centre, Nanjing University, Nanjing 210023, P. R. China. E-mail: zguo@nju.edu.cn; Fax: +86 25 83314502; Tel: +86 25 83594549

<sup>b</sup>State Key Laboratory of Pharmaceutical Biotechnology, School of Life Sciences, Nanjing University, Nanjing 210023, P. R. China. E-mail: boxwxy@nju.edu.cn; Fax: +86 25 83314502; Tel: +86 25 83594549

<sup>c</sup>School of Food Science and Engineering, Nanjing University of Finance & Economics, Nanjing 210023, P. R. China

† Electronic supplementary information (ESI) available: Experimental details, synthetic routes, NMR, UV-vis, HPLC, cyclic voltammogram, protein expression, acute toxicity and images of tumours. See DOI: 10.1039/d0sc00197j





expression of Mcl-1 in A549/DDP, A2780/DDP and CDDP-insensitive Caov3 cells is significantly higher than that in other cells (see Fig. S8†). Complexes 1 and 2 exhibited strong cytotoxicity towards all the tested cancer cells regardless of the Mcl-1 expression; whereas CDDP only showed high cytotoxicity against cancer cells expressing a low level of Mcl-1. The results highlighted the effectiveness of targeting Mcl-1 as a strategy for overcoming CDDP resistance.

### Cellular uptake

Owing to the potent cytotoxicity of 1 and 2 against CDDP-resistant cancer cells, the cellular Pt contents after incubation with A549/DDP cells for 12 h were measured by means of inductively coupled plasma mass spectrometry (ICP-MS). The results are shown in Fig. 2. The cellular Pt accumulation follows an order of  $2 > 1 > \text{CDDP}$ , which is in line with their lipophilicity and cytotoxicity sequences. Apparently, the conjugation of L<sub>1</sub> or L<sub>2</sub> with the Pt<sup>IV</sup> scaffold greatly improves the lipophilicity and cellular uptake of the complexes, which may contribute to the elevated cytotoxicity. Further, we measured the cellular Pt content in A549/DDP cells after incubation with different concentrations of CDDP, 1 and 2 for 36 h. The cellular uptake of Pt is positively correlated with the concentration of the complexes (see Table S3†). The Pt contents in A549/DDP cells after treatment with 12 μM CDDP, 1.4 μM 1, and 0.7 μM 2 are similar, suggesting that the cell-penetrating ability of 1 and 2 is greater than that of CDDP.

### DNA damage

DNA is believed to be the major cellular target of platinum complexes, so the ability of 1 and 2 to platinize nuclear DNA was assessed. After drug treatment, the genomic DNA of A549/DDP cells was extracted by a DNA isolation reagent (DNAzol) and the quantity of bound Pt was measured by ICP-MS. As shown in Fig. 3A, the platination of DNA by 1 and 2 is greater than that by CDDP, which may be due to the higher cellular uptake of 1 and 2 in A549/DDP cells. γ-H2AX, the

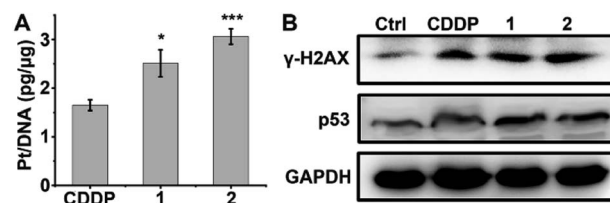


Fig. 3 Platination of cellular DNA (A), expression of γ-H2AX and p53 (B) in A549/DDP cells after incubation with 1 μM CDDP, 1 and 2 for 36 h. \*  $p < 0.05$ , \*\*\*  $p < 0.001$  (versus CDDP-treated group).

phosphorylated form of the histone protein H2AX, is a known biomarker of DNA DSBs caused by CDDP and can be detected by immunoblotting.<sup>46–48</sup> Fig. 3B shows that the expression of γ-H2AX in drug-treated A549/DDP cells increased significantly as compared with the control cells, indicating that the genomic DNA was severely damaged by the platinum complexes. The expression of p53, a downstream effector of DNA damage,<sup>49</sup> also increased after treatment with complexes 1, 2 or CDDP (Fig. 3B), suggesting that the DNA damage could not be repaired and that p53 began to initiate the apoptosis process.

### Cell cycle arrest

Cellular DNA damage could induce cell cycle arrest.<sup>43</sup> We hence examined the cell cycle arrest of A549/DDP cells by flow cytometry after treatment with the complexes. As shown in Fig. 4, in comparison with the control, the cell distribution in the S and G2 phases increased moderately after the treatment with 1 and 2. CDDP also arrested the cell cycle mainly in the S and G2 phases, which is consistent with other reports.<sup>43</sup> The similarity of the cell cycle arrest among these complexes suggests that the active form and DNA damage mode of 1 and 2 are similar to those of CDDP.

The results associated with cellular DNA damage response and cycle arrest demonstrate that complexes 1 and 2 were efficiently reduced in A549/DDP cells to release Pt<sup>II</sup> species for DNA binding, which constituted the basis for their remarkable cytotoxicity.

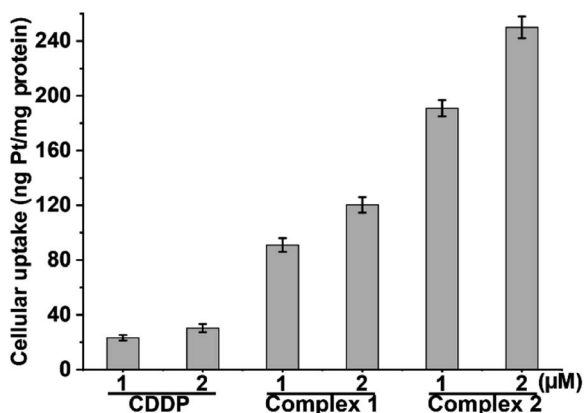


Fig. 2 Cellular uptake of Pt in A549/DDP cells after exposure to CDDP, 1 and 2 for 12 h.

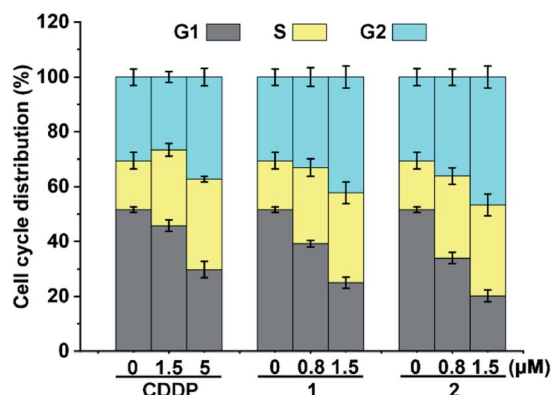


Fig. 4 Cell cycle arrest of A549/DDP cells after incubation with CDDP, 1 and 2 for 36 h.



### Expression of Mcl-1 and apoptotic proteins

In the absence of complexes, the expression of Mcl-1 in A549/DDP and A2780/DDP cells is significantly higher than that in A549 and A2780 cells (see Fig. S8†); hence, we examined the expression of Mcl-1 in A549/DDP cells in the presence of **1** or **2** using WB. As shown in Fig. 5A, the expression of Mcl-1 in A549/DDP cells is significantly inhibited, while it is slightly upregulated by CDDP as compared with the control cells. The downregulation of Mcl-1 could arise from the higher cellular uptake of **1** and **2** than that of CDDP (see Fig. 2). To examine this possibility, we studied the expression of Mcl-1 in A549/DDP cells after incubation with 1.4  $\mu\text{M}$  **1**, 0.7  $\mu\text{M}$  **2**, and 12  $\mu\text{M}$  CDDP, which ensured similar Pt accumulation in the cells (*vide supra*). The results show that the expression of Mcl-1 decreased after incubation with **1** and **2**, but increased after incubation with CDDP as compared with the control (see Fig. S11†), thus proving that the downregulation of cellular Mcl-1 by **1** and **2** is mainly due to the introduction of axial ligands rather than the higher cellular accumulation of Pt. Actually, ligand L<sub>1</sub> or L<sub>2</sub> alone could downregulate the cellular Mcl-1 at high concentrations (see Fig. S12†). The concentrations of **1** and **2** (*ca.* 1  $\mu\text{M}$ ) required to inhibit cellular Mcl-1 are much lower than those of L<sub>1</sub> and L<sub>2</sub> (*ca.* 200  $\mu\text{M}$ ), implying that it may be hard for the negatively charged ligands to enter the cells, and hence showing the advantages of **1** and **2** as integrated functional entities. In fact, the IC<sub>50</sub> values of the mixtures of CDDP and L<sub>1</sub> or L<sub>2</sub> are similar to that of CDDP (see Table 1), showing no superiority in cytotoxicity.

It is known that Mcl-1 prevents the activation of apoptosis effector proteins such as Bax, either through direct interaction or by inhibiting proapoptotic BH3-only proteins like Bim.<sup>50</sup> Therefore, the downregulation or inhibition of Mcl-1 could result in the activation of several proapoptotic proteins and facilitate the release of cytochrome c (Cyt c) into the cytosol, thereby activating caspase and triggering an apoptotic response.<sup>50</sup> The upregulation of Bim and Bax as well as the release of Cyt c in A549/DDP cells after treatment with **1** and **2** are shown in Fig. 5. The release of Cyt c can activate apoptotic protease and then cleave the caspase-3 zymogen, leading to apoptosis.<sup>51</sup> Therefore, we further measured the level of cleaved caspase-3 in A549/DDP cells after incubation with CDDP, **1**, and

**2**. As expected, cleaved caspase-3 was observed in cancer cells after the treatment with complexes **1** and **2** (see Fig. S13†). All these events are conducive to apoptosis or suppressing resistance to apoptosis.

### Apoptosis

The apoptosis of A549/DDP cells after treatment with these complexes for 72 h and staining with annexin V-FITC and propidium iodide (PI) was investigated. The cellular density plots are shown in Fig. 6. Complexes **1** and **2** efficiently induced 60.9% and 65.5% of A549/DDP cells to go into early apoptosis, respectively. By contrast, CDDP only triggered 2.7% of the cells to undergo early apoptosis, which agrees well with the CDDP-resistant characteristics of A549/DDP cells. The sharp contrast of **1** and **2** to CDDP in promoting apoptosis reveals that these Pt<sup>IV</sup> complexes possess great potential to conquer CDDP resistance.

### Expression of HR proteins RAD51 and BRCA2

In addition to the antiapoptotic function, Mcl-1 also plays a key role in the DNA damage response.<sup>52,53</sup> Cellular Mcl-1 depletion can impede the repair of DNA DSBs by impairing HR and decreasing the expression of related proteins.<sup>15</sup> RAD51 and BRCA2 play essential roles in HR by promoting homology search and stimulating strand invasion into the sister chromatid. Specifically, following DNA-end resection, BRCA2 directs RAD51 filament nucleation onto single-stranded DNA (ssDNA), which catalyzes a strand exchange reaction to initiate HR repair.<sup>54,55</sup> We hence measured the levels of RAD51 and BRCA2 in A549/DDP cells after exposure to complexes **1** and **2** or CDDP to evaluate their impact on the HR ability. As shown in Fig. 7, CDDP induced an increase in RAD51 expression, presumably due to the damage to genetic DNA, and barely influenced the

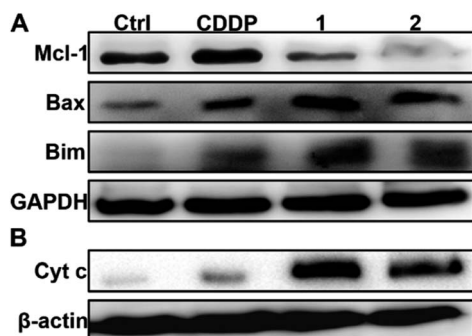


Fig. 5 Expression of Mcl-1, Bax and Bim (A), and Cyt c (B) in A549/DDP cells after incubation with complexes **1** and **2** (1  $\mu\text{M}$ ) for 36 h.

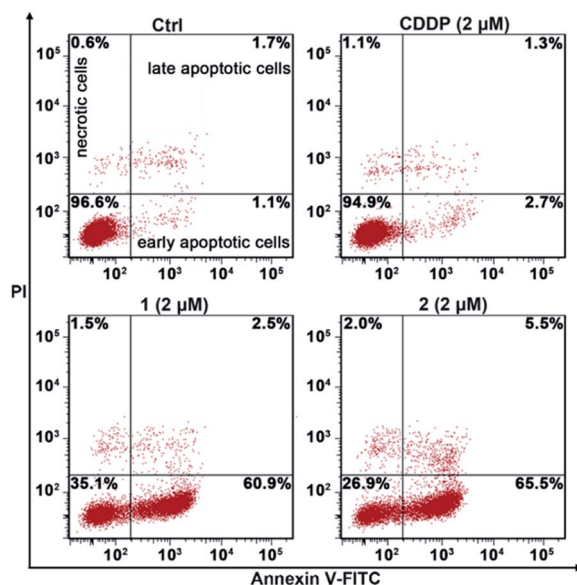


Fig. 6 Apoptotic analysis of A549/DDP cells by flow cytometry after incubation with the complexes for 72 h.



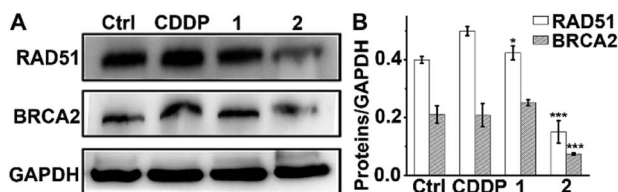


Fig. 7 Expression of RAD51 and BRCA2 in A549/DDP cells after incubation with each complex (1  $\mu\text{M}$ ) for 36 h (A), and the relative expression levels of RAD51 and BRCA2 to GAPDH (B). \*  $p < 0.05$ , \*\*\*  $p < 0.001$  (versus CDDP-treated group).

expression of BRCA2. The levels of RAD51 and BRCA2 in 1-treated cells were slightly higher than those in the control cells, suggesting that 1 had almost no effect on the expression of RAD51 and BRCA2. Impressively, the expression of RAD51 and BRCA2 decreased markedly after treatment with 2 as compared with both the control and CDDP-treated cells. The down-regulation of RAD51 implies that the repair of DSBs by HR is inactivated, and that DNA damage could remain to produce lethal effects to cancer cells. It has been reported that BRCA2-deficient cancer cells are hypersensitive to DNA-crosslinking agents such as CDDP due to the impaired HR, while BRCA2-proficient cancer cells are refractory to Pt-based drugs owing to the effective HR.<sup>56,57</sup> Knockdown of BRCA2 can enhance the cytotoxicity of CDDP in ovarian cancer cells.<sup>58</sup> Therefore, BRCA2 is a potential target for defeating CDDP resistance. The decreased expression of BRCA2 indicates that 2 can reduce the HR ability of A549/DDP cells. Oddly, complex 1 only differs slightly from complex 2 in terms of ligands, but it hardly influenced the expressions of RAD51 and BRCA2 in A549/DDP cells. Therefore, we suppose that the 6-methyl in L<sub>2</sub> may play a key role in suppressing the expression of these proteins; however, the detailed action is unknown at the moment. The results exemplify that even a minute change in the structure of Pt<sup>IV</sup> complexes could produce significant impact on their cytostatic mechanism and antitumor potency.

### Formation of RAD51 foci

Furthermore, immunofluorescence staining was used to study the formation of RAD51 foci, which is regarded as a critical

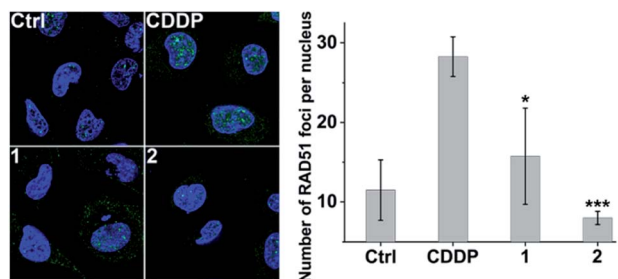


Fig. 8 Representative images of the formation of RAD51 foci (green) in the nucleus (blue) induced by different complexes (1  $\mu\text{M}$ ) after incubation with A549/DDP cells for 36 h (left), and the number of RAD51 foci per nucleus (right). \*  $p < 0.05$ , \*\*\*  $p < 0.001$  (versus CDDP-treated group).

step and functional biomarker in HR.<sup>59,60</sup> As shown in Fig. 8, CDDP triggered increased RAD51 foci (green) as compared with the control due to the DNA damage. However, the number of RAD51 foci in the nucleus induced by 2 is markedly less than that induced by CDDP even though the DNA damage caused by 2 is more severe than that caused by CDDP (see Fig. 3 and S9<sup>†</sup>). The results show that complex 2 can prevent the formation of RAD51 foci, which would hinder the HR repair of DSBs, and further sensitize cancer cells to DNA damage.

### Acute toxicity and *in vivo* antitumor activity

Finally, we evaluated the acute toxicity and *in vivo* antitumor efficacy of 1 and 2. The median lethal dose (LD<sub>50</sub>), body weight change and histological images of major organs after intravenous injection of each complex were investigated. The LD<sub>50</sub> values of 1 and 2 are  $16.24 \pm 2.89$  and  $12.31 \pm 1.31$  mg kg<sup>-1</sup>, respectively (see Fig. S14<sup>†</sup>), much higher than that of CDDP ( $4.06 \pm 1.02$  mg kg<sup>-1</sup>). No obvious change in body weight or damage to major organs was observed in the 1- or 2-treated mice (see Fig. S15 and S16<sup>†</sup>). By contrast, the CDDP-treated mice showed significant weight loss as compared with the control (see Fig. S15<sup>†</sup>). These results indicate that complexes 1 and 2 are less toxic to the body or more biocompatible than CDDP. Furthermore, mice implanted with A549 cells were used as xenograft models to evaluate the *in vivo* antitumor efficacy of 1 and 2. As shown in Fig. 9 and S17,<sup>†</sup> strong inhibition of tumor growth was observed after the treatment. On day 15, the average tumor volume was  $940.26 \pm 50.55$  and  $676.25 \pm 80.64$  mm<sup>3</sup> for the control and CDDP groups, respectively. Remarkably, complexes 1 and 2 effectively suppressed the tumor growth. The average tumor volume in the 1- and 2-treated groups after 15 d was  $189.82 \pm 43.17$  and  $67.29 \pm 6.71$  mm<sup>3</sup>, respectively, only reaching 20% and 7% of the control size. These results indicate that complexes 1 and 2 are more efficient inhibitors of tumor growth and less toxic to mice than CDDP, and hence are promising drug candidates for cancer therapy.

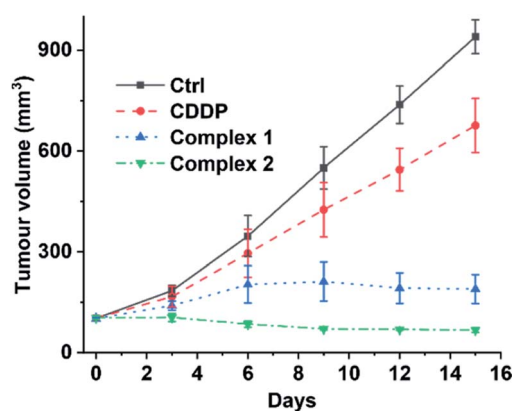


Fig. 9 Volume of A549 tumours in mice treated intravenously with CDDP (1.3 mg<sub>Pt</sub> kg<sup>-1</sup>), 1, and 2 (1.1 mg<sub>Pt</sub> kg<sup>-1</sup>) every three days for 15 d.





- 26 E. Gabano, M. Ravera, F. Trivero, S. Tinello, A. Gallina, I. Zanellato, M. B. Gariboldi, E. Monti and D. Osella, *Dalton Trans.*, 2018, **47**, 8268–8282.
- 27 Z. Xu, J. Zhao, S. Gou and G. Xu, *Chem. Commun.*, 2017, **53**, 3749–3752.
- 28 V. Reshetnikov, S. Daum and A. Mokhir, *Chem. – Eur. J.*, 2017, **23**, 5678–5681.
- 29 E. Petruzzella, J. P. Braude, J. R. Aldrich-Wright, V. Gandin and D. Gibson, *Angew. Chem., Int. Ed.*, 2017, **56**, 11539–11544.
- 30 S. H. Josef Mayr, B. Koblmüller, M. H. M. Klose, K. Holste, B. Fischer, K. Pelivan, W. Berger, P. Heffeter, C. R. Kowol and B. K. Keppler, *J. Biol. Inorg. Chem.*, 2017, **22**, 591–603.
- 31 Z. Wang, Z. Xu and G. Zhu, *Angew. Chem., Int. Ed.*, 2016, **55**, 15564–15568.
- 32 R. M. Gregory Thiabaud, G. He, J. F. Arambula, Z. H. Siddik and J. L. Sessler, *Angew. Chem., Int. Ed.*, 2016, **55**, 12626–12631.
- 33 D. Y. Q. Wong, J. H. Lim and W. H. Ang, *Chem. Sci.*, 2015, **6**, 3051–3056.
- 34 S. G. Awuah, Y. R. Zheng, P. M. Bruno, M. T. Hemann and S. J. Lippard, *J. Am. Chem. Soc.*, 2015, **137**, 14854–14857.
- 35 K. Suntharalingam, Y. Song and S. J. Lippard, *Chem. Commun.*, 2014, **50**, 2465–2468.
- 36 R. K. Pathak, S. Marrache, J. H. Choi, T. B. Berding and S. Dhar, *Angew. Chem., Int. Ed.*, 2014, **53**, 1963–1967.
- 37 Q. Cheng, H. Shi, H. Wang, Y. Min, J. Wang and Y. Liu, *Chem. Commun.*, 2014, **50**, 7427–7430.
- 38 J. Kasparkova, H. Kostrhunova, O. Novakova, R. Krikavova, J. Vanco, Z. Travnicek and V. Brabec, *Angew. Chem., Int. Ed.*, 2015, **54**, 14478–14482.
- 39 S. Zhang, H. Yuan, Y. Guo, K. Wang, X. Wang and Z. Guo, *Chem. Commun.*, 2018, **54**, 11717–11720.
- 40 A. Friberg, D. Vigil, B. Zhao, R. N. Daniels, J. P. Burke, P. M. Garcia-Barrantes, D. Camper, B. A. Chauder, T. Lee, E. T. Olejniczak and S. W. Fesik, *J. Med. Chem.*, 2013, **56**, 15–30.
- 41 J. L. Yap, L. Chen, M. E. Lanning and S. Fletcher, *J. Med. Chem.*, 2017, **60**, 821–838.
- 42 J. Z. Zhang, P. Bonnitcha, E. Wexselblatt, A. V. Klein, Y. Najajreh, D. Gibson and T. W. Hambley, *Chem. – Eur. J.*, 2013, **19**, 1672–1676.
- 43 Y. R. Zheng, K. Suntharalingam, T. C. Johnstone, H. Yoo, W. Lin, J. G. Brooks and S. J. Lippard, *J. Am. Chem. Soc.*, 2014, **136**, 8790–8798.
- 44 N. Muhammad, N. Sadia, C. Zhu, C. Luo, Z. Guo and X. Wang, *Chem. Commun.*, 2017, **53**, 9971–9974.
- 45 M. D. Hall, H. R. Mellor, R. Callaghan and T. W. Hambley, *J. Med. Chem.*, 2007, **50**, 3403–3411.
- 46 I. Revet, L. Feeney, S. Bruguera, W. Wilson, T. K. Dong, D. H. Oh, D. Dankort and J. E. Cleaver, *Proc. Natl. Acad. Sci. U. S. A.*, 2011, **108**, 8663–8667.
- 47 W. M. Bonner, C. E. Redon, J. S. Dickey, A. J. Nakamura, O. A. Sedelnikova, S. Solier and Y. Pommier, *Nat. Rev. Cancer*, 2008, **8**, 957–967.
- 48 S. Burma, B. P. Chen, M. Murphy, A. Kurimasa and D. J. Chen, *J. Biol. Chem.*, 2001, **276**, 42462–42467.
- 49 M. I. Sheau-Yann Shieh, Y. Taya and C. Prives, *Cell*, 1997, **91**, 325–334.
- 50 J. M. Adams and S. Cory, *Cell Death Differ.*, 2018, **25**, 27–36.
- 51 M. J. White, K. McArthur, D. Metcalf, R. M. Lane, J. C. Cambier, M. J. Herold, M. F. van Delft, S. Bedoui, G. Lessene, M. E. Ritchie, D. C. Huang and B. T. Kile, *Cell*, 2014, **159**, 1549–1562.
- 52 S. Jamil, C. Stoica, T. L. Hackett and V. Duronio, *Cell Cycle*, 2010, **9**, 2843–2855.
- 53 G. Chen, A. T. Magis, K. Xu, D. Park, D. S. Yu, T. K. Owonikoko, G. L. Sica, S. W. Satola, S. S. Ramalingam, W. J. Curran, P. W. Doetsch and X. Deng, *J. Clin. Invest.*, 2018, **128**, 500–516.
- 54 L. Ranjha, S. M. Howard and P. Cejka, *Chromosoma*, 2018, **127**, 187–214.
- 55 M. Roberti, F. Schipani, G. Bagnolini, D. Milano, E. Giacomini, F. Falchi, A. Balboni, M. Manerba, F. Farabegoli, F. De Franco, J. Robertson, S. Minucci, I. Pallavicini, G. Di Stefano, S. Giroto, R. Pellicciari and A. Cavalli, *Eur. J. Med. Chem.*, 2019, **165**, 80–92.
- 56 K. Gudmundsdottir and A. Ashworth, *Oncogene*, 2006, **25**, 5864–5874.
- 57 J. Han, C. Ruan, M. S. Y. Huen, J. Wang, A. Xie, C. Fu, T. Liu and J. Huang, *Nat. Commun.*, 2017, **8**, 1470.
- 58 B. Wan, L. Dai, L. Wang, Y. Zhang, H. Huang, G. Qian and T. Yu, *Endocr.-Relat. Cancer*, 2018, **25**, 69–82.
- 59 C. Cruz, M. Castroviejo-Bermejo, S. Gutierrez-Enriquez, A. Llop-Guevara, Y. H. Ibrahim, A. Gris-Oliver, S. Bonache, B. Morancho, A. Bruna, O. M. Rueda, Z. Lai, U. M. Polanska, G. N. Jones, P. Kristel, L. de Bustos, M. Guzman, O. Rodriguez, J. Grueso, G. Montalban, G. Caratu, F. Mancuso, R. Fasani, J. Jimenez, W. J. Howat, B. Dougherty, A. Vivancos, P. Nuciforo, X. Serres-Creixams, I. T. Rubio, A. Oaknin, E. Cadogan, J. C. Barrett, C. Caldas, J. Baselga, C. Saura, J. Cortes, J. Arribas, J. Jonkers, O. Diez, M. J. O'Connor, J. Balmana and V. Serra, *Ann. Oncol.*, 2018, **29**, 1203–1210.
- 60 M. Špirek, J. Mlčoušková, O. Belán, M. Gyimesi, G. M. Harami, E. Molnár, J. Novacek, M. Kovács and L. Krejci, *Nucleic Acids Res.*, 2018, **46**, 3967–3980.
- 61 R. G. Kenny and C. J. Marmion, *Chem. Rev.*, 2019, **119**, 1058–1137.
- 62 X. Wang, X. Wang and Z. Guo, *Acc. Chem. Res.*, 2015, **48**, 2622–2631.
- 63 N. Muhammad and Z. Guo, *Curr. Opin. Chem. Biol.*, 2014, **19**, 144–153.
- 64 D. Hanahan and R. A. Weinberg, *Cell*, 2011, **144**, 646–674.
- 65 R. Yamaguchi, L. Lartigue and G. Perkins, *Pharmacol. Ther.*, 2018, **195**, 13–20.
- 66 Y. Wan, N. Dai, Z. Tang and H. Fang, *Eur. J. Med. Chem.*, 2018, **146**, 471–482.

